ELSEVIER

Seminars in
ROENTGENOLOGY

Advanced MR Imaging of Musculoskeletal Tumors: An Overview

Lana Hirai Gimber, MD, MPH, Tyson S. Chadaz, MD, William Flake, BS, and Mihra S. Taljanovic, MD, PhD, FACR

Introduction

Musculoskeletal (MSK) tumors are a heterogeneous group of bone and soft tissue neoplasms. Initial MSK tumor imaging workup relies on radiographs (Fig. 1a), which are essential in the evaluation of MSK bone lesions and even if negative may add to the evaluation of soft tissue tumors. Correlation with clinical findings is also of great importance.[1] Due to their complexity, these tumors require complex, multi-disciplinary treatment strategies to achieve optimal local control and avoid metastatic spread.

Magnetic resonance (MR) imaging plays a major role in the workup and treatment of MSK tumors, with the first magnetic resonance imagining (MRI) machines becoming commercially available in the 1980s.[2] It frequently represents the imaging modality of choice in detection and characterization of MSK tumors, provides evaluation of tumor extent, guidance to treatment planning, and is crucial in post-treatment assessment and surveillance.

Anatomical imaging such as T1-weighted fat sensitive sequences, fluid-sensitive sequences, and delayed postcontrast T1-weighted fat-suppressed (FS) sequences are used routinely in clinical practice in the MRI evaluation of MSK tumors. However, some studies have shown that these routine anatomical MR sequences are not able to accurately characterize many MSK lesions.[3,4]

Many institutions are now implementing advanced MR imaging techniques for the workup and follow-up of MSK tumors.[5-8] These sequences interrogate tissues at a cellular level and include diffusion-weighted imaging, chemical shift imaging, dynamic contrast enhancement (DCE), and MR spectroscopy. While these sequences can provide essential information and add to the specificity of the radiology diagnosis, they must be interpreted in conjunction with the routine anatomical imaging sequences. This article aims to help radiologists become familiar with functional MR imaging of MSK tumors, identify which functional MR imaging techniques would be helpful in different situations, and discuss limitations and technical considerations when employing functional MR imaging in these settings.

Routine Anatomical MSK Tumor Imaging

T1-Weighted Sequences

Nonenhanced spin-echo T1-weighted MR sequences without FS typically serve as the mainstay in assessment of bone marrow replacement or intraosseous extension of neoplasm (Fig. 1b).[5,6,9] They provide excellent topographic assessment of the examined regions. In addition, T1-weighted sequences can reveal information regarding internal content of a lesion. For example, lesions containing macroscopic fat such as a liposarcoma frequently have increased intrinsic T1 signal. However, the majority of both malignant and benign MSK tumors show intermediate (isointense to skeletal muscle) to low signal intensity on these sequences which is frequently nonspecific.

Fluid-Sensitive Sequences

Both short tau inversion recovery and T2-weighted FS sequences are routinely used to evaluate MSK tumors. These sequences optimize contrast between fluid and surrounding tissues, giving essential information regarding the relationship between tumor and surrounding vital structures (Fig. 1c).[5,6,9,10] Short tau inversion recovery

Department of Medical Imaging, Banner University Medical Center, The University of Arizona, College of Medicine, Tucson, AZ.
Conflicts of interest: none.
This research did not receive any specific grant from funding agencies in the public, commercial, or not-for-profit sectors.
Address reprint requests to Lana Hirai Gimber, MD, MPH, Arizona State Radiology, 2492 E River Rd, Tucson, AZ 85718
E-mail: lana.hirai.gimber@gmail.com

https://doi.org/10.1053/j.ro.2018.10.001

sequences can be helpful to avoid heterogeneous fat suppression, which can occur frequently in MR imaging of MSK masses in the extremities.[11] Intermediate-weighted proton-density FS sequences are sometimes preferred over T2-weighted FS sequences due to increased signal-to-noise ratio.[11] T2-weighted sequences without FS are also used by some radiologists for assessing the nature of the mass by comparing signal intensities of muscle, fat, and fluid.[11] In addition, similar to T1-weighted sequences, fluid-sensitive sequences can also reveal information regarding internal content of a lesion. For example, lesions with a high myxoid component or cystic lesions typically demonstrate increased intrinsic fluid-sensitive signal.

Static Delayed Postcontrast T1-Weighted Sequences, Gradient-Echo With Isotropic Resolution, and Digital Subtraction

T1-weighted FS postcontrast sequences are crucial to identify areas that exhibit contrast enhancement and tumor extent (Fig. 1d). Three-dimensional gradient-echo sequences with isotropic resolution can be substituted in effort to decrease overall scan time, as they can be acquired in a single plane and then reformatted into other planes. Notably, the gradient echo sequences are frequently suboptimal in patients with metal implants due to profound susceptibility artifact, which is frequently seen in patients with limb salvage prostheses. However, many available metal reduction techni-

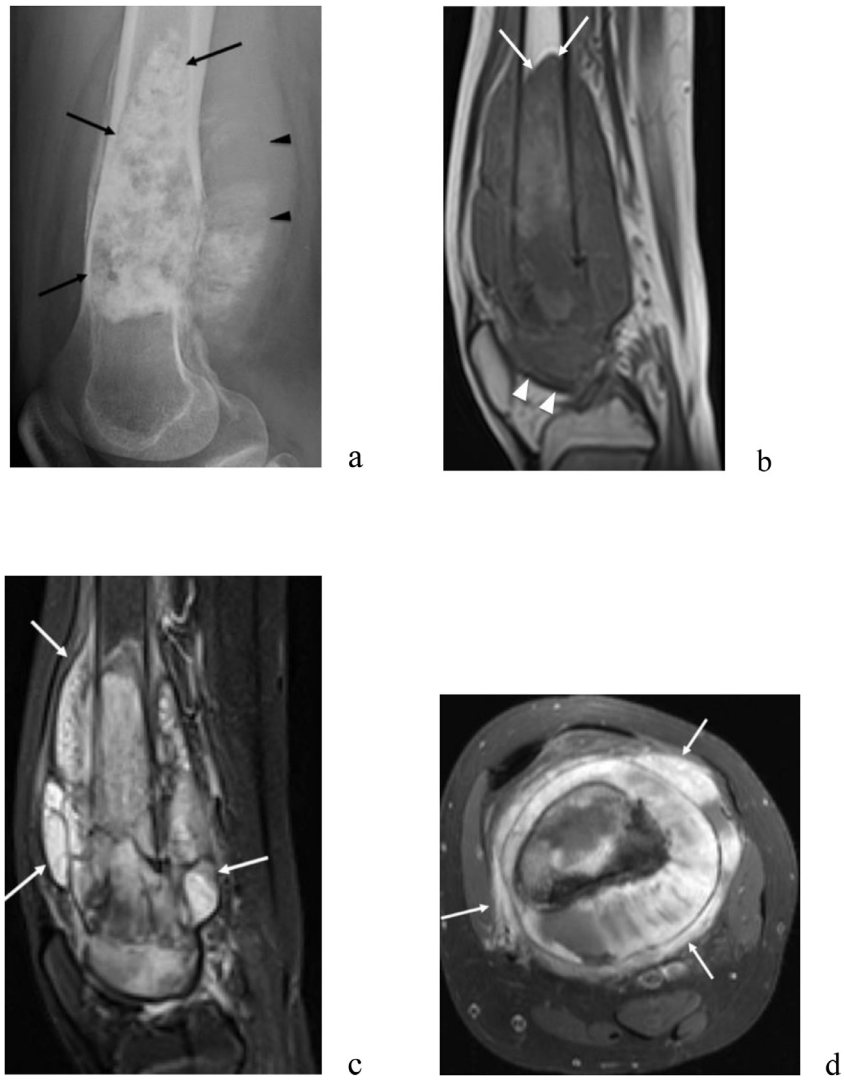

Figure 1 Twelve-year-old female with osteosarcoma of the distal left femur. (a) Lateral radiograph demonstrates a destructive intramedullary lesion (arrows) within the distal femur containing osseous matrix with large posterior soft tissue component (arrowheads). (b) Sagittal T1-weighted MR image of the same area highlights the extent of medullary involvement proximally to the femoral mid shaft (arrows) and distally into the knee joint (arrowheads). (c) Sagittal STIR MR image of the same region highlights the contrast between the lesion and surrounding soft tissues (arrows). (d) Axial static delayed T1 fat-suppressed (FS) postcontrast MR image of the distal femur further highlights areas of contrast enhancement and tumor extent (arrows).

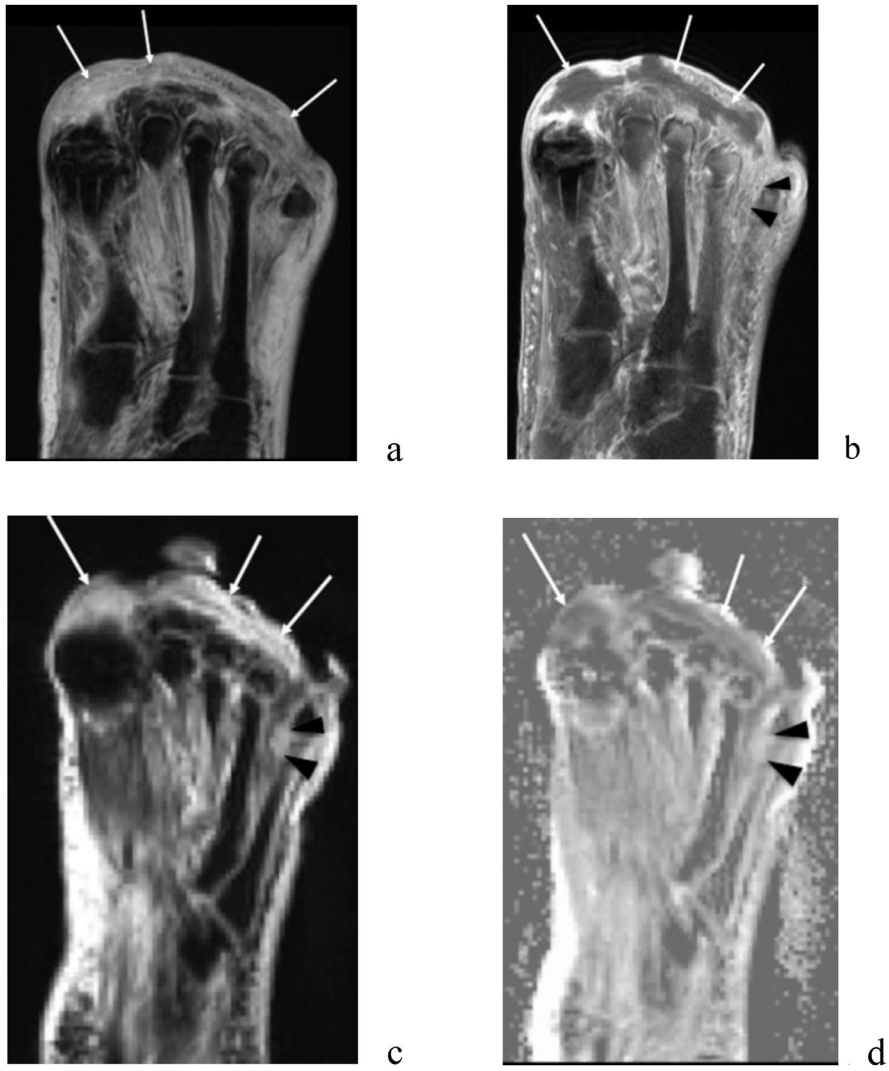

Figure 2 Seventy-year-old female with pain and purulent drainage of the left foot after falling and found to have a soft tissue abscess. (a) Axial STIR image of the left foot demonstrates confluent high signal intensity edema within the soft tissues at the plantar aspect of the first through fifth toes (arrows). (b) Axial static postcontrast T1 FS image demonstrates peripherally enhancing fluid collection in the same region (arrows) consistent with an abscess. (c, d) Axial trace (mean diffusivity) diffusion-weighted MR image (c) and apparent diffusion coefficient (ADC) map (d) demonstrate restricted diffusion within the lesion (arrows in c and d), as evidenced by high signal on the trace image and low signal areas on the ADC map. Note additional heterogeneously enhancing subcutaneous edema consistent with cellulitis (b) shows high signal on trace (c) and ADC map diffusion-weighted (d) MR images consistent with T2 shine-through phenomenon (arrowheads in c and d).

ques have been described, with several advanced MR imaging acquisition technologies available.[12,13] Some of these techniques are vendor specific including "VAT" (view angle tilting), Syngo "WRAP" (metal artifact reduction techniques in MRI), and "Semac" (slice encoding for metal artifact correction) from Siemens, "MAVRIC" (multiacquisition variable-resonance image combination) from General Electric, and "MARS" (Metal artifact reduction sequence) from Phillips.[13]

Further, digital image subtraction, a technique in which the enhanced images are subtracted from the unenhanced images, can be performed in cases where there is a question of subtle contrast enhancement.

Advanced Imaging Techniques

Diffusion-Weighted Imaging

Diffusion-weighted imaging (DWI) measures the Brownian motion of molecules in tissues.[14] Intracellular movement of water is more restricted when compared to molecules more freely diffusing in extracellular free water. Therefore, more cellular tissues will have increased inhibition of molecular diffusion. Hence, DWI has been used as a marker to gauge the degree of cellularity or cellular integrity, with more cellular areas, such as expected in tumors, demonstrating restricted diffusion.[15] As reviewed previously by Ahlawat and Fayad, DWI can help aid in characterization of soft tissue

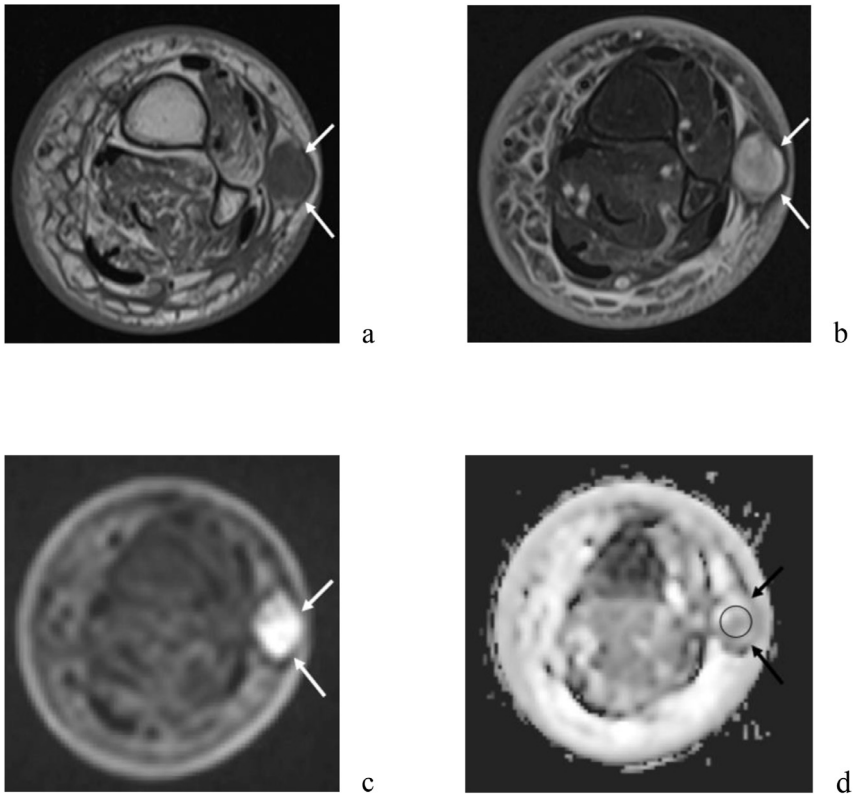

Figure 3 Eighty-one-year-old female with history of sclerosing rhabdomyosarcoma involving the dorsal left foot status post resection and radiation, presenting with a new metastatic lesion in the leg. Patient was unable to receive intravenous contrast. (a) Axial T1-weighted MR image demonstrates a rounded lesion isointense to muscle within the subcutaneous tissues and abutting the superficial fascia at the anterolateral aspect of the distal leg (arrows). (b) Axial T2-weighted FS MR image demonstrates heterogeneous high signal intensity within the lesion (arrows). (c, d) Axial trace diffusion-weighted MR image (c) and ADC map (d) demonstrate restricted diffusion within the lesion (arrows in c and d), as evidenced by high signal on the trace image and low signal areas on the ADC map. The minimum ADC value (circle in d) was found to be 0.94×10^{-3} mm^2/s. Surgical resection was performed with pathology proven metastatic rhabdomyosarcoma.

masses as benign vs malignant, cystic vs solid, abscesses vs postoperative fluid collections, recurrent disease vs nodular scar, and areas of viable tumor vs post-treatment necrosis.[15]

Diffusion-sensitizing gradient strengths, or b-values, are used to describe the magnitude of sensitivity to Brownian motion, with at least 2 different b-values normally used. The individual source images are combined into a single trace image for interpretation. In addition, they are used to generate the apparent diffusion coefficient (ADC) map, which is the slope of exponential decrease in signal intensities between the different b-values.[5,6] At the authors' institution, similar to other protocols published,[6] b-values of 50, 400, and 800 s/mm^2 are used. The lowest b-value of 50 s/mm^2 has been used previously in order to reduce the contribution of blood perfusion, which can affect ADC measurements.[16] The trace image is used in conjunction with the ADC map, which may be interpreted using qualitative or quantitative methods.

For the qualitative method of interpreting DWI sequences, one visually assesses if restricted diffusion is present. This would manifest as high signal intensity on trace images with corresponding low signal in this area on the ADC map. While the qualitative method of restricted diffusion may be helpful in identifying more cellular areas in a tumor, we have used this method most in identifying soft tissue abscesses when no contrast-enhanced MR imaging sequences are available (Fig. 2), as an abscess will demonstrate restricted diffusion.[17] Lesions with a very high T2 relaxation time that do not have true restricted diffusion appear bright on both the trace image and the ADC map, a phenomenon known as T2 shine through (Fig. 2).[18]

Lower ADC values are reflective of more cellular areas.[19] A region of interest (ROI) is drawn and the minimum, mean, and maximum ADC measurements can be obtained. Although some studies have explored manual methods of ADC measurements,[20-22] there is currently no standard procedure for the size or placement of the ROI, which can be a potential cause of inter-reader variability. At the authors' institution, the ROI is placed within the lesion with the lowest visual signal on the ADC map. It is of importance to include the largest possible area within the lesion while being careful to exclude surrounding extralesional tissues.[16,20,23,24]

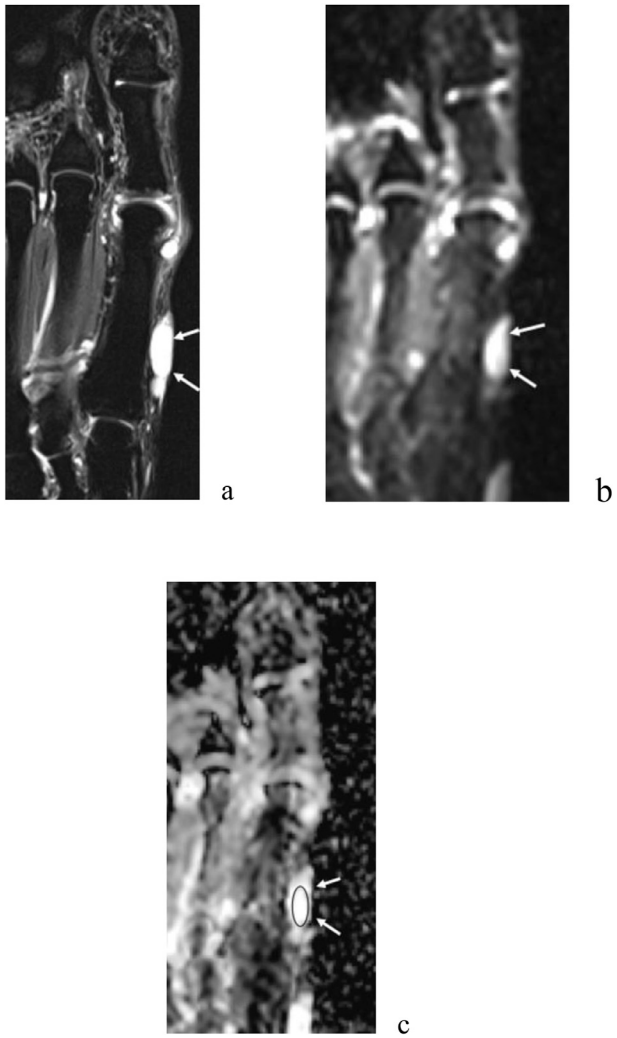

Figure 4 Sixty-nine-year-old female with great toe soft tissue ganglion. Patient was unable to obtain contrast. (a) Axial T2-weighted FS MR image of the medial forefoot demonstrates a lobulated high signal intensity lesion (arrows) within the subcutaneous tissues at the medial aspect of the first metatarsal. (b) Axial trace MR image demonstrates high signal within the lesion (arrows). (c) ADC map image demonstrates no corresponding low signal to suggest restricted diffusion (arrows). Mean ADC value (circle in c) was found to be 2.6×10^{-3} mm^2/s, most consistent with a benign cystic lesion.

Multiple studies have explored DWI in evaluating soft tissue masses, with promising results published regarding the use of minimum ADC values (Fig. 3). Using minimum ADC values with noncontrast routine, MR sequences has been found to have equal diagnostic accuracy compared to static contrast-enhanced MR sequences for discriminating benign from malignant soft tissue tumors.[24] Different minimum ADC cutoff values have been suggested in the literature. A study by Demehri et al found that a minimum ADC equal to or less than 1.0×10^{-3} mm^2/s and tumor diameter more than 4.2 cm resulted in 100% sensitivity in distinguishing malignant vs benign peripheral nerve sheath tumors.[23] Another study by Del Grande et al reported that a mass is 6 times more likely to be malignant if it has a minimum ADC $\leq 0.8 \times 10^{-3}$ mm^2/s.[24]

In addition, using the mean ADC can be helpful in cases of soft tissue cystic lesions (Fig. 4). A study by Subhawong et al found a mean ADC value of greater than 2.5×10^{-3} mm^2/s yielded 80% sensitivity and 100% specificity for classifying a high fluid-signal intensity soft tissue mass as a cyst, distinguishing a high fluid content solid tumor from a cyst without postcontrast sequences.[25]

However, while promising results have been published regarding minimum ADC values and soft tissue masses, varying results have been published regarding the mean ADC in predicting malignancy, and caution should be taken when using this value. Overlap in mean ADC between benign and malignant soft tissue tumors has been shown,[26] especially in the setting of soft tissue myxomas and malignant myxoid tumors.[27,28]

DWI results in the assessment of bone lesions have been mixed. A prior study[29] suggested that qualitative DWI may be helpful in differentiating benign pelvic skeletal lesions from malignant lesions, although no significant differences were seen with quantitative ADC values. In comparison, another study that explored the accuracy of quantitative DWI to characterize intramedullary lesions as benign or malignant found higher ADC values in benign lesions, with minimum ADC as providing the highest accuracy.[16] In this study, a threshold minimum ADC value of 0.9×10^{-3} mm^2/s had a sensitivity of 92% and 78% specificity for differentiating benign and malignant lesions.[16] However, overlap of ADC values was seen in biologically aggressive benign lesions and malignant lesions, possibly reflecting their underlying aggressive biologic behavior and cellularity. In addition, caution should be taken when evaluating chondroid matrix lesions, as a study demonstrated that ADC values could not distinguish between enchondroma and chondrosarcoma of any grade, or low vs high grade chondrosarcoma.[30] Current literature supports the value of F-18 2-[fluorine-18]fluoro-2-deoxy-d-glucose (FDG) Positron emission tomography (PET) in differentiation of benign from malignant chondroid neoplasms[31] and future use of PET MR imaging may be of value.

The role of DWI in grading post-treatment response of MSK tumors has also been explored. Prior studies and review articles suggest higher ADC ratios in osteosarcoma patients, who have good response vs poor response post chemotherapy.[32,33] A recent review discussed that some studies have shown an increase in ADC value post-treatment in multiple myeloma lesions around 4-6 weeks, although timing of the post-treatment assessment appears crucial with return of normal marrow fat and decrease in ADC value as time progressed.[34] Similarly, another study has suggested that ADC values have a high degree of correlation with tumor volumes after anticancer therapy in subjects with soft tissue sarcomas, although in this study the imaging intervals were too heterogeneous for analysis regarding treatment period length.[35]

DWI has many advantages as part of the MSK tumor protocol. In addition to the added information it can provide, the

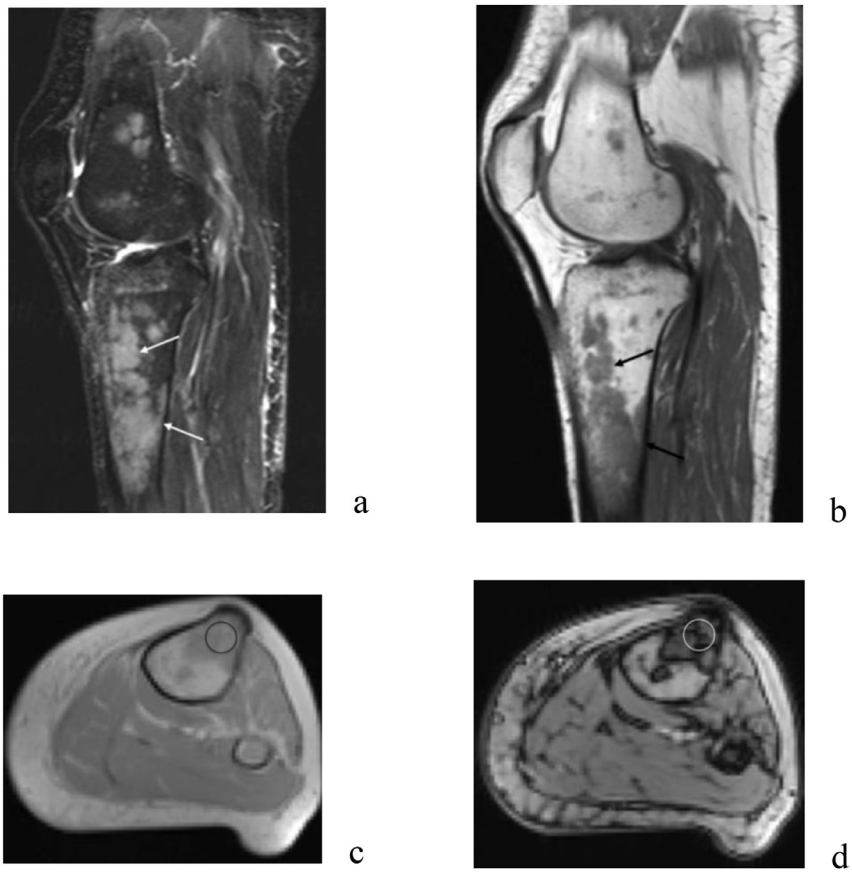

Figure 5 Fifty-year-old male with remote history of carcinoma with left knee pain, and incidentally found focal areas of prominent red marrow reconversion. (a) Sagittal STIR MR image demonstrates focal confluent high to intermediate signal lesions within the distal femur and proximal tibia (arrows). Sagittal T1-weigthed MR image demonstrates corresponding low signal (arrows) within these regions concerning for a marrow replacing process. (c, d) Axial in-phase (c) and opposed-phase (d) MR images through the area of marrow replacement in the proximal tibia demonstrate greater than 20% signal drop from 427 on the in-phase image (circle in c) to 251 on the opposed-phase image (circle in d) most consistent with red marrow. Similar measurements were obtained in the other lesion areas and there were no findings concerning for malignancy.

sequence can be performed relatively quickly, does not require intravenous contrast, and allows quantitative assessment. However, as a Gradient echo (GRE) technique, DWI is not reliable in the evaluation of very small subcentimeter lesions, and is susceptible to artifacts such as hardware and air. Therefore, the DWI sequence should always be interpreted in conjunction with the routine anatomical sequences.

Chemical Shift Imaging

Chemical shift imaging, or in-phase and opposed-phase imaging, allow sensitive identification of fat within bone marrow. When fat and water are contained in a single voxel, they will cancel each other out on the opposed-phase sequences and reinforce each other on the in-phase sequences due to their inherent differences in precession frequencies. Therefore, signal loss within the bone marrow on the opposed-phase sequence when compared to the in-phase sequence confirms the presence of fat. At the authors' institution, typical TR/TE for long bones on 1.5T are 220/4.7 milliseconds for in-phase and 220/2.3 milliseconds for opposed-phase; on 3T typical TR/TE values are 180/2.46 milliseconds for in-phase and 180/1.23 milliseconds for opposed-phase.

As described by Fayad et al,[6] this sequence can distinguish between an infiltrative marrow replacing tumor from hematopoietic marrow or bone marrow edema. Bone marrow, including hematopoietic red marrow, contains both water and fat and therefore drops in signal intensity on the opposed-phase imaging (Fig. 5). In contrast, osseous tumors replace the normal marrow and do not demonstrate significant drop in signal intensity on the opposed-phase imaging (Fig. 6).

This drop in signal can be measured quantitatively as the percentage change in signal intensity on the opposed-phase sequence relative to the in-phase sequence. A systematic review and meta-analysis performed by Thawait et al[36] demonstrated that the strongest predictor in differentiating benign from malignant fractures was a 20% signal drop on

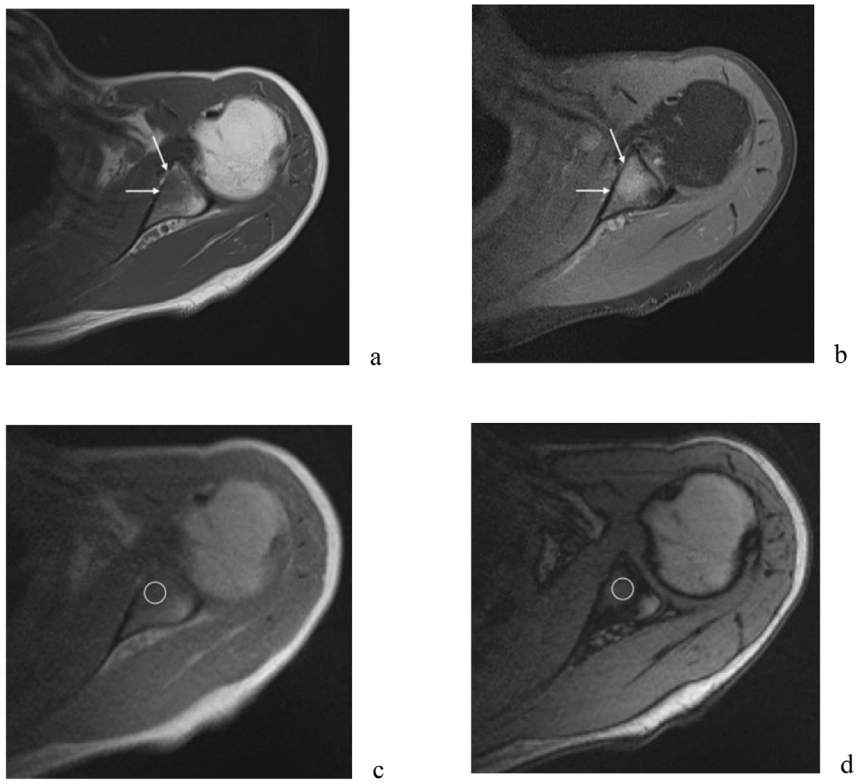

Figure 6 Fifty-four-year-old female with remote history of retroperitoneal liposarcoma and pathology proven metastatic lesion in the left glenoid. (a) Axial T1-weighted MR image of the left shoulder demonstrates a bone marrow replacing process (arrows) at the anterior aspect of the glenoid. (b) Axial proton density FS MR image in the same location demonstrates high signal within the lesion (arrows). (c, d) Axial in-phase (c) and opposed-phase (d) MR images demonstrate less than 20% signal drop from 90 on the in-phase image (circle in c) to 82 on the opposed-phase image (circle in d) in the lesion highly concerning for malignancy.

the opposed phase images. Another study demonstrated a sensitivity of over 91% and specificity of 73% using this cut-off value of 20%.[37] Similar results have also been seen in the pelvis.[38] Using this cut-off value of 20% could eliminate the need for biopsy in a large number of patients with otherwise indeterminate bone lesions.

Exploring chemical shift imaging on 3T, a recent study found that a 25% threshold of signal drop can be used for differentiating benign from malignant bone marrow replacing lesions, providing 100% sensitivity and at least 86% specificity.[39]

Similar to DWI, chemical shift imaging requires no intravenous contrast. One consideration when performing this sequence is to obtain the opposed-phase at the shorter TE than the in-phase sequence when acquiring on a 3T MRI. A prior study demonstrated a high false-negative rate for red marrow when the opposed-phase was acquired at the longer echo time.[40]

Dynamic Contrast Enhanced MR Imaging

DCE, or perfusion imaging, evaluates exchanges of intravascular contrast and extravascular space.[41] Previously described in the literature,[6,42] it is a rapid, volumetric, and GRE sequence that covers a volume of interest repeatedly after intravenous contrast is administered, allowing characterization of the enhancement of the tissues. The underlying principle is that the rapid arterial enhancement should be seen in malignant tissue due to increased perfusion at a microscopic level. DCE can be helpful in distinguishing malignant vs benign MSK neoplastic lesions, tumor recurrence vs postoperative nodular scar, and post-treatment response.[8,24,42-48]

The suggested MR imaging protocol for DCE of MSK tumors has been previously published.[6] Intravenous gadolinium-based contrast agent is injected at a rate of 2-5 mL/sec. Imaging takes approximately 3-5 minutes with a temporal resolution of about 5-15 seconds, depending on the spatial resolution and field of view.

DCE can be evaluated using both qualitative and quantitative methods.[49] At the authors' institution, the qualitative method is used. The lesion enhancement is evaluated and compared to the enhancement of adjacent arteries and veins to determine whether enhancement is early arterial, late arterial, or venous. A semiquantitative measurement is available which generates time-to-intensity curves from an ROI,[5,6,41] with multiple parameters extracted from these graphs using commercial software. An absolute quantitative measurement relies on pharmacokinetic modeling to quantify tumor blood flow, microvasculature, and capillary permeability,[41] although technically demanding and not ready for routine clinical practice.

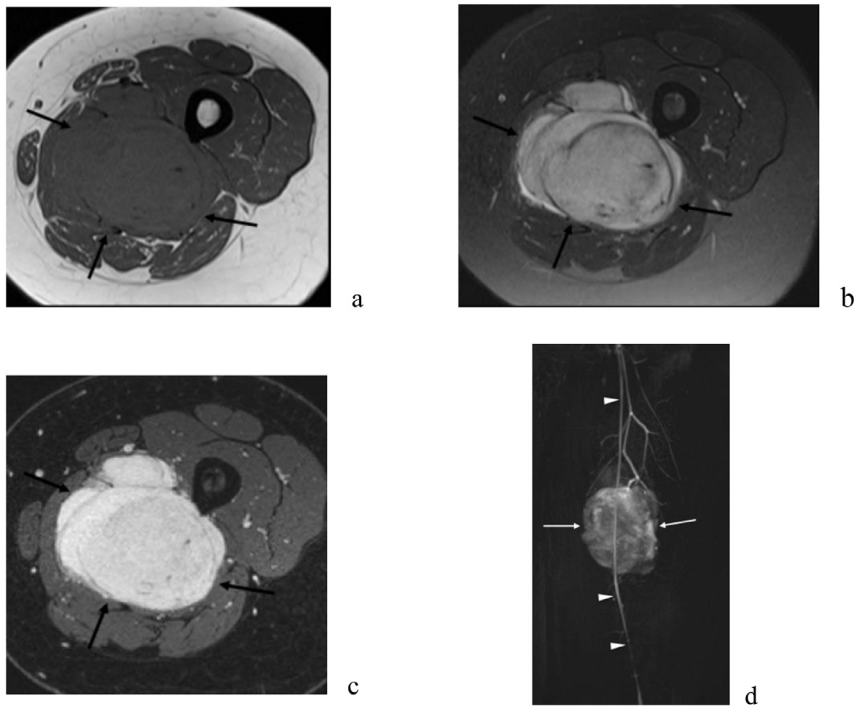

Figure 7 Twenty-two-year-old female with leg mass and pain who was found to have a pathology proven malignant peripheral nerve sheath tumor. (a) Axial T1-weighted MR image demonstrates an isointense to muscle large intramuscular soft tissue mass (arrows) at the posterior aspect of the thigh abutting the femoral cortex. (b) Axial T2-weighted FS MR image demonstrates mildly heterogeneous increased signal within the lesion (arrows). (c) Axial static postcontrast MR image demonstrates relatively uniform avid enhancement within the lesion (arrows). (d) Coronal dynamic contrast enhanced (DCE) T1−weighted 3D FS Volumetric Interpolated Breathhold Examination (VIBE) MR image demonstrates early arterial enhancement of the lesion (arrows), with enhancement of the surrounding arteries (arrowheads) consistent with malignancy.

Multiple studies have analyzed DCE in the setting of MSK tumors. Prior studies have demonstrated increased prediction of malignant lesions with the addition of DCE sequences, as malignant lesions tend to show early arterial enhancement[24,43,44] (Figs. 7 and 8). In the setting of post-treatment and surveillance imaging, DCE has also been shown to play a crucial role. While recurrence, nodular scar, fibrosis, granulation tissue, and postradiation changes all show enhancement on static delayed contrast enhanced images and are at times indistinguishable on this sequence, DCE can be helpful in this area. On the DCE sequence, post-operative soft tissue recurrence would most likely demonstrate early arterial enhancement, while benign entities such as nodular scar would not (Fig. 9). A study by Del Grande et al demonstrated that the addition of DCE MR sequence increases the specificity for detection of recurrent disease to 97% vs 52% with only static post-contrast enhancement sequences.[45] Multiple additional studies have found DCE to be a potential predictor for response to treatment,[8,42,47,48] with one in particular having demonstrated that early rapidly progressive enhancement correlated histologically with residual viable tumor, while late and gradual or absence of enhancement was associated with necrosis or granulation tissue.[46]

DCE can add valuable information with little additional scan time, especially since static postcontrast enhanced sequences are usually also obtained. Pitfalls to DCE include poor spatial resolution and susceptibility to artifacts. In addition, some older studies have demonstrated that patterns of contrast enhancement in benign and malignant lesions have been shown to overlap and lack of typical enhancement patterns have been seen in some lesions.[23,50,51]

MR Spectroscopy

MR spectroscopy is currently used primarily in the research setting. This technique adds molecular characterization of tumors without the addition of intravenous contrast. In this technique, an ROI is selected and the water, lipid, and other metabolite frequencies are shown, with the amplitude of these frequencies proportional to the metabolite concentration.[41,52] This theoretically provides a noninvasive method of distinguishing malignant vs nonmalignant tissues based on certain biochemicals that have been established as markers of malignancy. Two types of MR spectroscopy are available, proton MR spectroscopy and phosphorus MR spectroscopy.[52] Proton MR spectroscopy is more commonly used in the MSK system and more easily integrated into clinical practice.[41,52]

Malignant lesions may have higher choline-containing compounds, as these are constituents of the phospholipid metabolism of cell membranes.[53,54] MR spectroscopy can

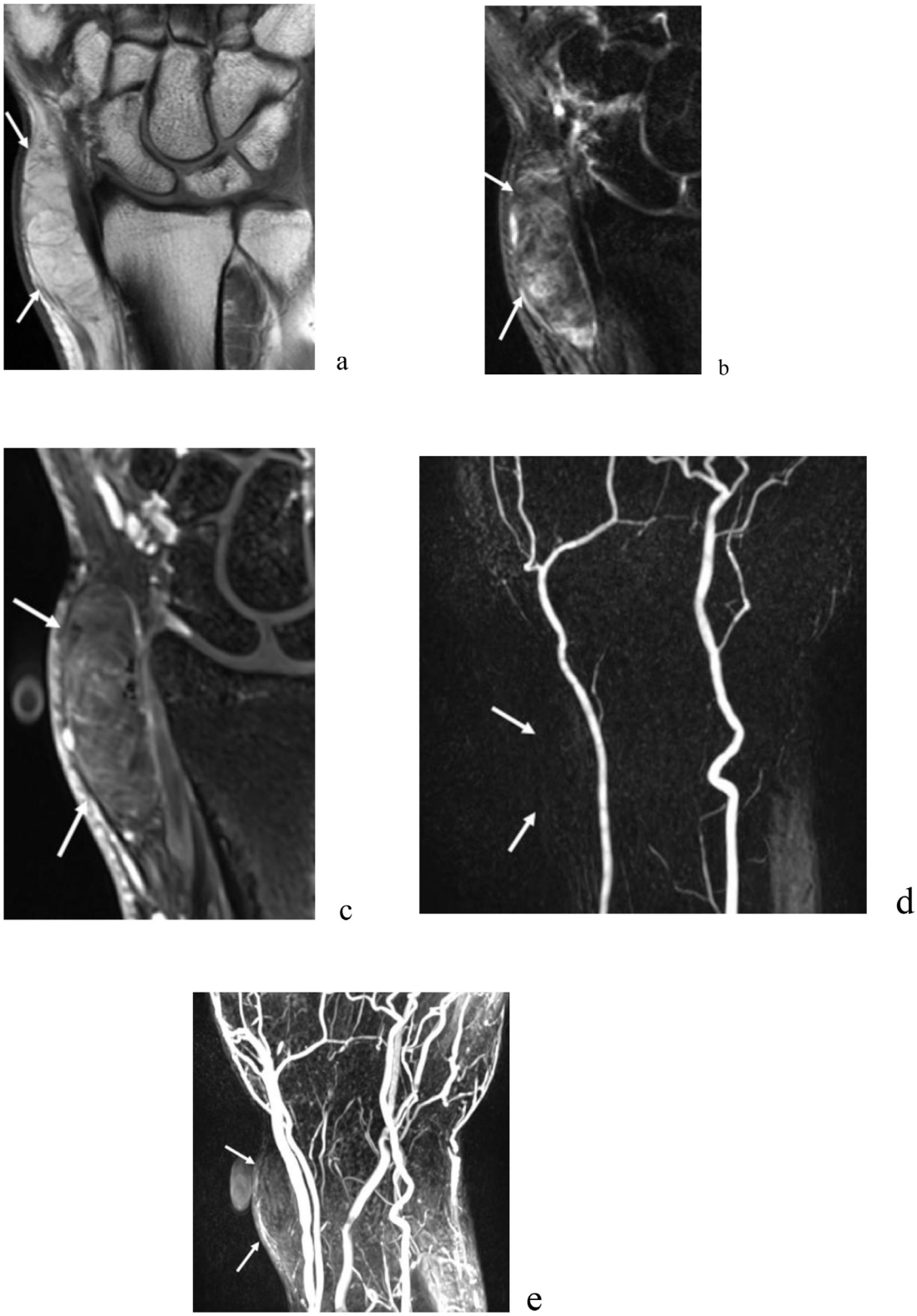

Figure 8 Fifty-seven-year-old male with pathology proven hemosideric fibrohistiocytic lipomatous soft tissue lesion in his wrist which is presumably benign. (a) Coronal T1-weighted MR image of the wrist demonstrates a mildly heterogeneous, predominantly high signal intensity lesion (arrows) within the subcutaneous tissues at the radial aspect of the wrist. Internal architecture of the lesion is more complex than that of the surrounding subcutaneous fat, concerning for malignancy. (b) Coronal T2-weighted FS MR image demonstrates heterogeneous areas of high signal within the lesion (arrows). (c) Coronal T1-weighted FS static postcontrast MR image demonstrates mild heterogeneous enhancement within the lesion (arrows), concerning for malignancy. (d) Coronal DCE MR image in the early arterial phase demonstrates no enhancement of the lesion (arrows). (e) Coronal DCE MR image in the venous phase demonstrates heterogeneous internal enhancement of the lesion (arrows) which is most consistent with a benign lesion.

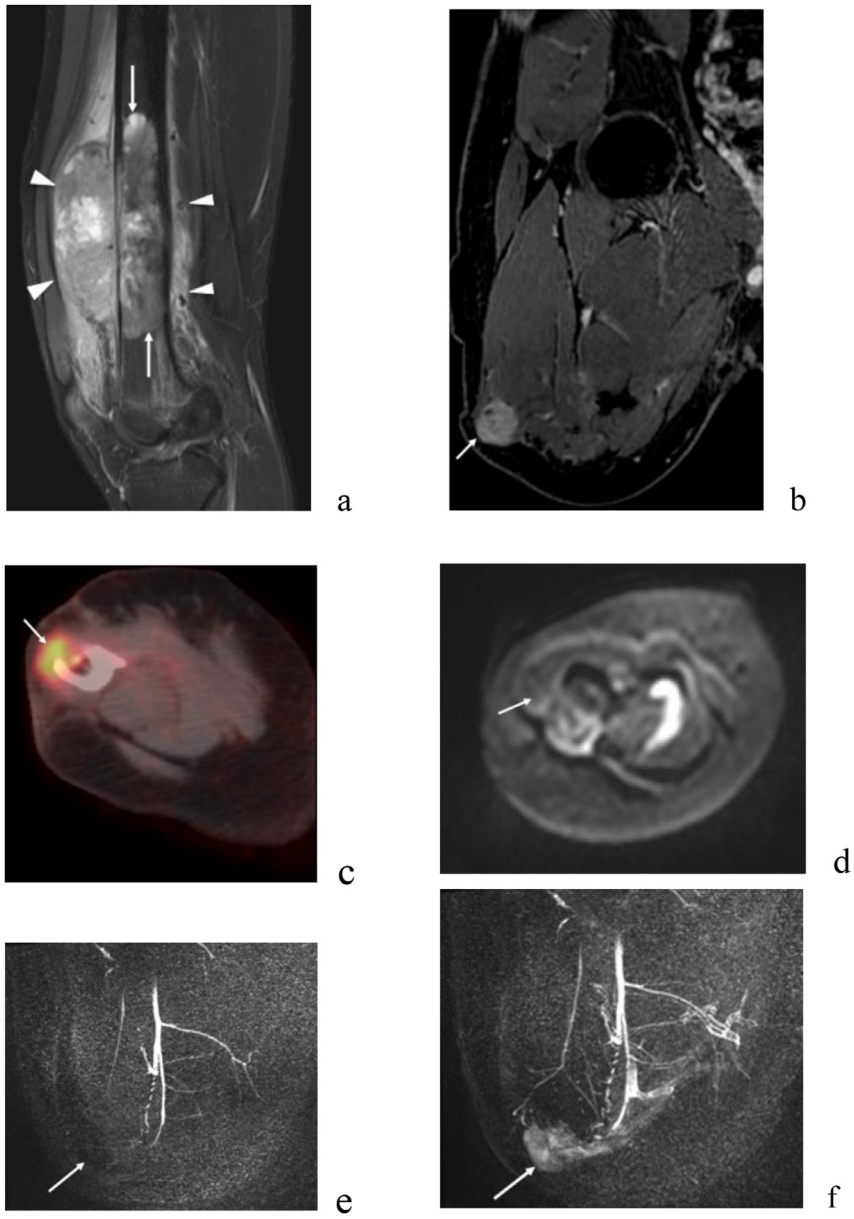

Figure 9 Seventeen-year-old male with history of distal femoral osteosarcoma status post above knee amputation with concern for tumor recurrence on follow-up imaging 2 years after surgery. (a) Preoperative sagittal STIR MR image demonstrates an aggressive heterogeneous, bone marrow replacing intramedullary lesion (arrows) within the distal femur with anterior and posterior soft tissue components (arrowheads) and surrounding soft tissue edema consistent with osteosarcoma. (b) Follow-up static post contrast T1-weighted FS coronal MR image after above knee amputation demonstrates a nodular area of enhancement (arrow) at the amputation site concerning for tumor recurrence. (c) Concurrent fused axial PET-CT image demonstrates increased radiotracer uptake in the same region (arrow), also concerning for tumor recurrence. (d) Axial trace MR image demonstrates no restricted diffusion in the area of concern (arrow). (e, f) Coronal DCE MR image in arterial phase (e) demonstrates no early arterial enhancement of the lesion. However, on the coronal DCE MR image in venous phase (f), there is venous enhancement (arrows). Diffusion-weighted and DCE MR images were most consistent with a benign etiology. Biopsy was negative for malignancy with the area of nodular enhancement representing a collapsed bursa.

detect these compounds using single voxel or multi voxel techniques.[52,53] Qualitatively, the presence of choline peaks or qualitative choline ratios can be used. Quantitative measurements of choline can also be obtained.

Some studies and review articles have shown that the metabolite choline has the potential to differentiate malignant from benign lesions.[6,54-59] A review performed by Subhawong et al demonstrated 88% sensitivity and 68% specificity in detection of malignancy using the choline peak, with increased accuracy when absolute choline quantification was used.[58] However, choline peaks have also been found in some benign tumors (Fig. 10).[59,60]

There are some technical drawbacks to MR spectroscopy. Manual shimming is needed to overcome field inhomogeneity

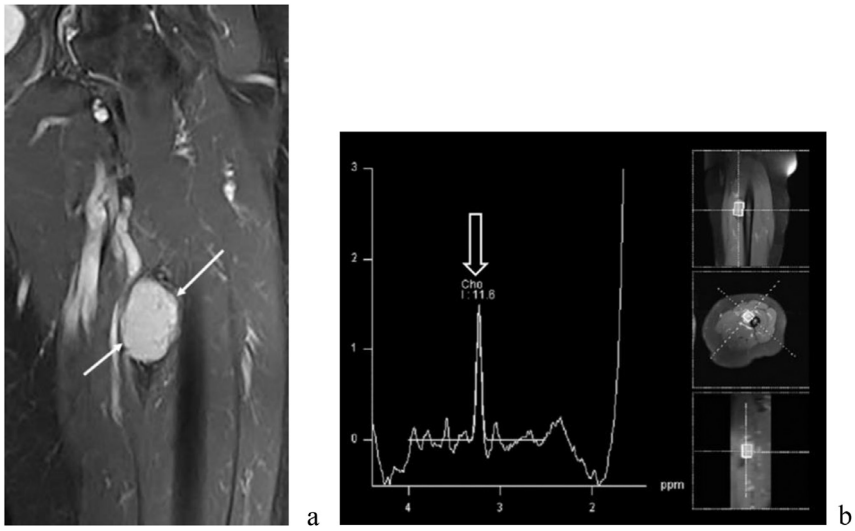

Figure 10 Fifty-eight-year-old female with incidental painless mass found in the thigh during a massage. (a) Coronal static postcontrast T1-weighted FS MR image demonstrates a uniformly enhancing rounded intermuscular mass (arrows) at the medial aspect of the proximal left thigh. (b) Proton MR spectroscopy imaging obtained at 3T with a TE of 144 ms with single voxel (rectangular outline) technique in the mass shows a prominent 3.2 ppm choline peak (arrow). Note that the lipid peak is partially visualized, extending beyond the limits of the display. Despite this choline peak, 2 biopsies demonstrated a benign nerve sheath tumor. It was unchanged in size on 2-year follow-up MR imaging. Images courtesy of Mark Krandsdorf, MD.

issues, which is technically complex.[52] The technique is time consuming, which limits its use to the research arena. When drawing ROIs, the largest region should be drawn to obtain the most data, however areas of calcification, fat, or vascular structures should be avoided due to obscuration of metabolic peaks of interest or signal drop-out.[52,58,61]

Conclusion

MSK neoplasms are a complex and heterogeneous group of tumors, which require a multidisciplinary treatment strategy. Conventional MR imaging offers information complementary to radiography that is essential in tumor workup and is invaluable in post-treatment assessment and surveillance. Functional MR imaging can add to the specificity of interpretations, however, these sequences must always be interpreted in conjunction with routine anatomical imaging sequences. It is important to understand which functional MR imaging techniques would be helpful in different situations, and to recognize limitations and technical considerations when employing these techniques.

Acknowledgments

The authors would like to thank Dr. Laura M Fayad from Johns Hopkins University School of Medicine for her guidance in initiation of advanced MSK tumor imaging protocols at our institution.

The authors would also like to thank Dr. Mark J. Kransdorf from Mayo Clinic for the MR spectroscopy images used in this manuscript.

References

1. Taljanovic MS, Hunter TB, Fitzpatrick KA, et al: Musculoskeletal magnetic resonance imaging: Importance of radiography. Skeletal Radiol 32:403-411, 2003
2. Tretkoff E: July, 1977: MRI uses fundamental physics for clinical diagnosis. APS News 15:2, 2018. July 2006
3. Crim JR, Seeger LL, Yao L, et al: Diagnosis of soft-tissue masses with MR imaging: Can benign masses be differentiated from malignant ones. Radiology 185:581-586, 1992
4. Moulton JS, Blebea JS, Dunco DM, et al: MR imaging of soft-tissue masses: Diagnostic efficacy and value of distinguishing between benign and malignant lesions. AJR Am J Roentgenol 164:1191-1199, 1995
5. Ahlawat S, Fayad LM: De novo assessment of pediatric musculoskeletal soft tissue tumors: Beyond anatomic imaging. Pediatrics 136:e194-e202, 2015
6. Fayad LM, Jacobs MA, Wang X, et al: Musculoskeletal tumors: How to use anatomic, functional, and metabolic MR techniques. Radiology 265:340-356, 2012
7. Garner HW, Kransdorf MJ: Musculoskeletal sarcoma: Update on Imaging of the post-treatment patient. Can Assoc Radiol J 67:12-20, 2016
8. Soldatos T, Ahlawat S, Montgomery E, et al: Multiparametric assessment of treatment response in high-grade soft-tissue sarcomas with anatomic and functional mr imaging sequences. Radiology 278:831-840, 2016
9. Pettersson H, Gillespy T, Hamlin DJ, et al: Primary musculoskeletal tumors: examination with MR imaging compared with conventional modalities. Radiology 164:237-241, 1987
10. Wetzel LH, Levine E, Murphey MD: A comparison of MR imaging and CT in the evaluation of musculoskeletal masses. Radiographics 7:851-874, 1987
11. Kransdorf MJ, Murphey MD: Imaging of soft-tissue musculoskeletal masses: Fundamental concepts. Radiographics 36:1931-1948, 2016
12. Koch KM, Bhave S, Gaddipati A, et al: Multispectral diffusion-weighted imaging near metal implants. Magn reson Med 79:987-993, 2018
13. Taljanovic MS, Gimber LH, Omar IM, et al: Imaging of postoperative infection at the knee joint. Semin musculoskeletal radiol 22:464-480, 2018
14. Koh DM, Collins DJ: Diffusion-weighted MRI in the body: Applications and challenges in oncology. AJR Am J Roentgenol 188:1622-1635, 2007

15. Ahlawat S, Fayad LM: Diffusion weighted imaging demystified: The technique and potential clinical applications for soft tissue imaging. Skeletal Radiol 47:313-328, 2018
16. Ahlawat S, Khandheria P, Subhawong TK, et al: Differentiation of benign and malignant skeletal lesions with quantitative diffusion weighted MRI at 3T. Eur J Radiol 84:1091-1097, 2015
17. Chun CW, Jung JY, Baik JS, et al: Detection of soft-tissue abscess: Comparison of diffusion-weighted imaging to contrast-enhanced MRI. J Magn Reson Imaging: JMRI 47:60-68, 2018
18. Chavhan GB, Alsabban Z, Babyn PS: Diffusion-weighted imaging in pediatric body MR imaging: Principles, technique, and emerging applications. Radiographics 34:E73-E88, 2014
19. Schnapauff D, Zeile M, Niederhagen MB, et al: Diffusion-weighted echo-planar magnetic resonance imaging for the assessment of tumor cellularity in patients with soft-tissue sarcomas. J Magn Reson Imaging JMRI 29:1355-1359, 2009
20. Ahlawat S, Khandheria P, Del Grande F, et al: Interobserver variability of selective region-of-interest measurement protocols for quantitative diffusion weighted imaging in soft tissue masses: Comparison with whole tumor volume measurements. J Magn Reson Imaging JMRI 43:446-454, 2016
21. Kwee RM, Dik AK, Sosef MN, et al: Interobserver reproducibility of diffusion-weighted MRI in monitoring tumor response to neoadjuvant therapy in esophageal cancer. PloS ONE 9:e92211, 2014
22. Lambregts DM, Beets GL, Maas M, et al: Tumour ADC measurements in rectal cancer: Effect of ROI methods on ADC values and interobserver variability. Eur Radiol 21:2567-2574, 2011
23. Demehri S, Belzberg A, Blakeley J, et al: Conventional and functional MR imaging of peripheral nerve sheath tumors: Initial experience. AJNR Am J Neuroradiol 35:1615-1620, 2014
24. Del Grande F, Ahlawat S, Subhangwong T, et al: Characterization of indeterminate soft tissue masses referred for biopsy: What is the added value of contrast imaging at 3.0 tesla. J Magn Reson Imaging JMRI 45:390-400, 2017
25. Subhawong TK, Durand DJ, Thawait GK, et al: Characterization of soft tissue masses: Can quantitative diffusion weighted imaging reliably distinguish cysts from solid masses. Skeletal Radiol 42:1583-1592, 2013
26. Einarsdottir H, Karlsson M, Wejde J, et al: Diffusion-weighted MRI of soft tissue tumours. Eur Radiol 14:959-963, 2004
27. Maeda M, Matsumine A, Kato H, et al: Soft-tissue tumors evaluated by line-scan diffusion-weighted imaging: Influence of myxoid matrix on the apparent diffusion coefficient. J Magn Reson Imaging JMRI 25:1199-1204, 2007
28. Nagata S, Nishimura H, Uchida M, et al: Diffusion-weighted imaging of soft tissue tumors: Usefulness of the apparent diffusion coefficient for differential diagnosis. Radiat Med 26:287-295, 2008
29. Douis H, Davies MA, Sian P: The role of diffusion-weighted MRI (DWI) in the differentiation of benign from malignant skeletal lesions of the pelvis. Eur J radiol 85:2262-2268, 2016
30. Douis H, Jeys L, Grimer R, et al: Is there a role for diffusion-weighted MRI (DWI) in the diagnosis of central cartilage tumors. Skeletal Radiol 44:963-969, 2015
31. Subhawong TK, Winn A, Shemesh SS, et al: F-18 FDG PET differentiation of benign from malignant chondroid neoplasms: A systematic review of the literature. Skeletal Radiol 46:1233-1239, 2017
32. Oka K, Yakushiji T, Sato H, et al: The value of diffusion-weighted imaging for monitoring the chemotherapeutic response of osteosarcoma: a comparison between average apparent diffusion coefficient and minimum apparent diffusion coefficient. Skeletal Radiol 39:141-146, 2010
33. Kubo T, Furuta T, Johan MP, et al: Value of diffusion-weighted imaging for evaluating chemotherapy response in osteosarcoma: A meta-analysis. Mol Clin Oncol 7:88-92, 2017
34. Dutoit JC, Verstraete KL: Whole-body MRI, dynamic contrast-enhanced MRI, and diffusion-weighted imaging for the staging of multiple myeloma. Skeletal Radiol 46:733-750, 2017
35. Dudeck O, Zeile M, Pink D, et al: Diffusion-weighted magnetic resonance imaging allows monitoring of anticancer treatment effects in patients with soft-tissue sarcomas. J Magn Reson Imaging JMRI 27:1109-1113, 2008
36. Thawait SK, Marcus MA, Morrison WB, et al: Research synthesis: What is the diagnostic performance of magnetic resonance imaging to discriminate benign from malignant vertebral compression fractures? Systematic review and meta-analysis. Spine 37:E736-E744, 2012
37. Douis H, Davies AM, Jeys L, et al: Chemical shift MRI can aid in the diagnosis of indeterminate skeletal lesions of the spine. Eur Radiol 26:932-940, 2016
38. Kohl CA, Chivers FS, Lorans R, et al: Accuracy of chemical shift MR imaging in diagnosing indeterminate bone marrow lesions in the pelvis: Review of a single institution's experience. Skeletal Radiol 43:1079-1084, 2014
39. Kumar NM, Ahlawat S, Fayad LM: Chemical shift imaging with in-phase and opposed-phase sequences at 3 T: What is the optimal threshold, measurement method, and diagnostic accuracy for characterizing marrow signal abnormalities. Skeletal Radiol 2018. https://doi.org/10.1007/s00256-018-2999-0. [Epub ahead of print]
40. Del Grande F, Subhawong T, Flammang A, et al: Chemical shift imaging at 3 Tesla: Effect of echo time on assessing bone marrow abnormalities. Skeletal Radiol 43:1139-1147, 2014
41. Teixeira PA, Beaumont M, Gabriela H, et al: Advanced techniques in musculoskeletal oncology: perfusion, diffusion, and spectroscopy. Semin Musculoskeletal Radiol 19:463-474, 2015
42. Fayad LM, Mugera C, Soldatos T, et al: Technical innovation in dynamic contrast-enhanced magnetic resonance imaging of musculoskeletal tumors: An MR angiographic sequence using a sparse k-space sampling strategy. Skeletal Radiol 42:993-1000, 2013
43. De Coninck T, Jans L, Sys G, et al: Dynamic contrast-enhanced MR imaging for differentiation between enchondroma and chondrosarcoma. Eur Radiol 23:3140-3152, 2013
44. van Rijswijk CS, Geirnaerdt MJ, Hogendoorn PC, et al: Soft-tissue tumors: value of static and dynamic gadopentetate dimeglumine-enhanced MR imaging in prediction of malignancy. Radiology 233:493-502, 2004
45. Del Grande F, Subhawong T, Weber K, et al: Detection of soft-tissue sarcoma recurrence: Added value of functional MR imaging techniques at 3.0 T. Radiology 271:499-511, 2014
46. van Rijswijk CS, Geirnaerdt MJ, Hogendoorn PC, et al: Dynamic contrast-enhanced MR imaging in monitoring response to isolated limb perfusion in high-grade soft tissue sarcoma: Initial results. Eur Radiology 13:1849-1858, 2003
47. Meyer JM, Perlewitz KS, Hayden JB, et al: Phase I trial of preoperative chemoradiation plus sorafenib for high-risk extremity soft tissue sarcomas with dynamic contrast-enhanced MRI correlates. Clin Cancer Res 19:6902-6911, 2013
48. Huang W, Beckett BR, Tudorica A, et al: Evaluation of soft tissue sarcoma response to preoperative chemoradiotherapy using dynamic contrast-enhanced magnetic resonance imaging. Tomography 2:308-316, 2016
49. Subhawong TK, Wilky BA: Value added: Functional MR imaging in management of bone and soft tissue sarcomas. Curr Opin Oncol 27:323-331, 2015
50. Erlemann R, Reiser MF, Peters PE, et al: Musculoskeletal neoplasms: static and dynamic Gd-DTPA-enhanced MR imaging. Radiology 171:767-773, 1989
51. Barile A, Regis G, Masi R, et al: Musculoskeletal tumours: Preliminary experience with perfusion MRI. La Radiologia Medica 112:550-561, 2007
52. Deshmukh S, Subhawong T, Carrino JA, et al: Role of MR spectroscopy in musculoskeletal imaging. Indian J Radiol Imaging 24:210-216, 2014
53. Fayad LM, Barker PB, Bluemke DA: Molecular characterization of musculoskeletal tumors by proton MR spectroscopy. Semin Musculoskeletal Radiol 11:240-245, 2007
54. Fayad LM, Bluemke DA, McCarthy EF, et al: Musculoskeletal tumors: Use of proton MR spectroscopic imaging for characterization. J Magn Reson Imaging JMRI 23:23-28, 2006
55. Fayad LM, Wang X, Salibi N, et al: A feasibility study of quantitative molecular characterization of musculoskeletal lesions by proton MR spectroscopy at 3 T. AJR Am J Roentgenol 195:W69-W75, 2010

56. Fayad LM, Barker PB, Jacobs MA, et al: Characterization of musculoskeletal lesions on 3-T proton MR spectroscopy. AJR Am J Roentgenol 188 (6):1513-1520, 2007
57. Kransdorf MJ, Bridges MD: Current developments and recent advances in musculoskeletal tumor imaging. Semin musculoskeletal Radiol 17:145-155, 2013
58. Subhawong TK, Wang X, Durand DJ, et al: Proton MR spectroscopy in metabolic assessment of musculoskeletal lesions. AJR Am J Roentgenol 198:162-172, 2012
59. Russo F, Mazzetti S, Grignani G, et al: In vivo characterisation of soft tissue tumours by 1.5-T proton MR spectroscopy. Eur Radiol 22:1131-1139, 2012
60. Wang CK, Li CW, Hsieh TJ, et al: Characterization of bone and soft-tissue tumors with in vivo 1H MR spectroscopy: initial results. Radiology 232:599-605, 2004
61. Teixeira PA, Hossu G, Kauffmann F, et al: Influence of calcium on choline measurements by 1H MR spectroscopy of thigh muscles. Eur Radiol 24:1309-1319, 2014